

Problems of Double Charm Production in e^+e^- Annihilation at $\sqrt{s} = 10.6$ GeV

Kui-Yong Liu ^(a) Zhi-Guo He ^(a) and Kuang-Ta Chao ^(b,a)

(a) Department of Physics, Peking University, Beijing 100871, People's Republic of China

(b) China Center of Advanced Science and Technology (World Laboratory), Beijing 100080, People's Republic of China

Abstract

Using the nonrelativistic QCD(NRQCD) factorization formalism, we calculate the color-singlet cross sections for exclusive production processes $e^+ + e^- \rightarrow J/\psi + \eta_c$ and $e^+ + e^- \rightarrow J/\psi + \chi_{cJ}$ ($J = 0, 1, 2$) at the center-of-mass energy $\sqrt{s}=10.6$ GeV. The cross sections are estimated to be 5.5fb, 6.7fb, 1.1fb, and 1.6fb for $\eta_c, \chi_{c0}, \chi_{c1}$ and χ_{c2} respectively. The calculated $J/\psi\eta_c$ production rate is smaller than the recent Belle data by about an order of magnitude, indicating the failure of perturbative QCD calculation to explain the double charmonium production data. In addition, we also calculate the χ_{c0} inclusive double charm production cross section of $e^+ + e^- \rightarrow \chi_{c0} + c\bar{c}$ in perturbative QCD and find that its value, which should be much larger than, is however saturated by the calculated cross sections of $e^+ + e^- \rightarrow J/\psi + \chi_{c0}$ plus $e^+ + e^- \rightarrow \psi(2S) + \chi_{c0}$. This again indicates that the perturbative QCD calculation for the charmonium (e.g. χ_{c0}) inclusive double charm production seriously underestimates the production rates, and nonperturbative QCD effects have to be considered at low energies such as $\sqrt{s}=10.6$ GeV.

PACS number(s): 12.40.Nn, 13.85.Ni, 14.40.Gx

Heavy quarkonium production is interesting in understanding both perturbative and non-perturbative quantum chromodynamics (QCD). In recent years the charmonium production has been studied in various processes, such as in hadron-hadron collision, electron-proton collision, fixed target experiments, B meson decays, as well as Z^0 decays. Among them, the study of charmonium production in e^+e^- annihilation is particularly interesting in testing the quarkonium production mechanisms, the color-singlet model and the color-octet model in the nonrelativistic QCD (NRQCD)[1] approach. This is not only because of the simpler parton structure involved in this process, which may be helpful in reducing the theoretical uncertainty, but also because of the spectacular experimental prospect opened up by the two B factories with BaBar and Belle, which will allow a fine data analysis for charmonium production with more than 10^8 e^+e^- annihilation events in the continuum at $\sqrt{s}=10.6$ GeV.

Recently the Belle Collaboration has reported the observation of prompt J/ψ via double $c\bar{c}$ production from the e^+e^- continuum[2]. For these results, not only the large fraction of the inclusive J/ψ production due to the double $c\bar{c}$ production is puzzling[3], but also the exclusive production rate of $J/\psi\eta_c$, $\sigma(e^+e^- \rightarrow J/\psi\eta_c(\gamma)) \times \mathcal{B}(\eta_c \rightarrow \geq 4\text{charged}) = (0.033_{-0.006}^{+0.007} \pm 0.009)\text{pb}$, may not be consistent with both the previous calculations[4, 5], which gave a cross section of a few pb for $J/\psi\eta_c$. In fact, recent perturbative estimates of the $J/\psi c\bar{c}$ cross section are only about 0.07 pb[6, 7, 8]. So the calculations of exclusive cross sections for e^+e^- annihilation into $J/\psi\eta_c$ and other double charmonium states such as $J/\psi\chi_{cJ}$ ($J = 0, 1, 2$) will be useful to clarify the problem. Experimentally, aside from $e^+e^- \rightarrow$

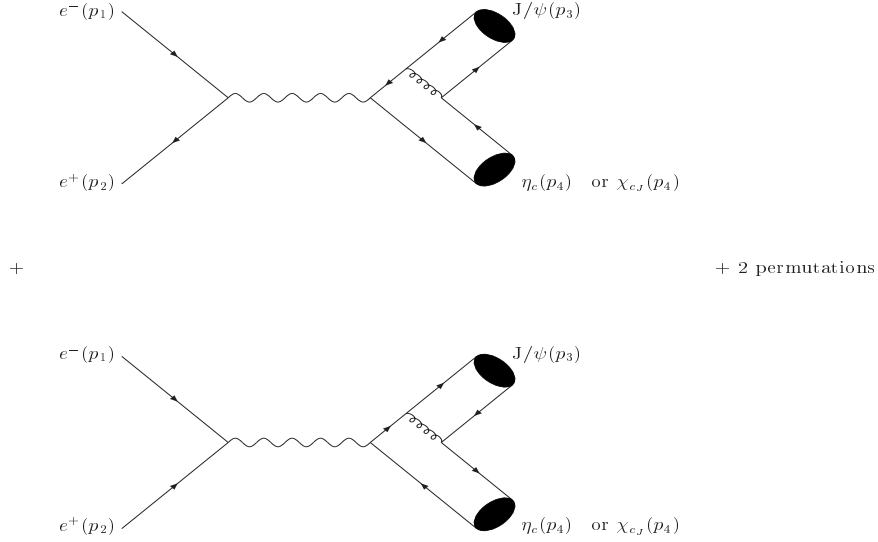


Figure 1: Feynman diagrams for $e^+e^- \rightarrow J/\psi + \eta_c(\chi_{cJ})$.

$J/\psi\chi_{c0}$ [2], Belle [10] has also studied processes $e^+e^- \rightarrow \chi_{c1}X$ and $e^+e^- \rightarrow \chi_{c2}X$, so we hope that the double charmonia production involving $\chi_{cJ}(J = 0, 1, 2)$ will be detectable in the near future. In the following we will calculate the cross sections $\sigma(e^+ + e^- \rightarrow J/\psi + \eta_c)$ and $\sigma(e^+ + e^- \rightarrow J/\psi + \chi_{cJ})$ in the leading order perturbative QCD. To this order ($\sim \alpha_s^2$) the color-singlet channel is dominant since all color-octet channels are of high order of v , which is the relative velocity of the charm quark and anti-charm quark in the charmonium, and therefore suppressed. Furthermore, in order to compare inclusive production with exclusive production rates associated with the χ_{cJ} charmonium states, we will calculate the cross section $\sigma(e^+ + e^- \rightarrow \chi_{c0} + c\bar{c})$, and this will again reveal the failure of perturbative QCD calculation for the charmonium inclusive production at $\sqrt{s}=10.6$ GeV.

We now write down the scattering amplitude which describes the creation of two color-singlet $Q\bar{Q}$ pairs in the e^+e^- annihilation process in Fig. 1 as

$$\begin{aligned}
\mathcal{A}(a + b \rightarrow Q\bar{Q}({}^{2S_\psi+1}L_{J_\psi})(P_3) + Q\bar{Q}({}^{2S+1}L_J)(P_4)) &= \sum_{L_{\phi z} S_{\psi z} s_1 s_2} \sum_{jk} \sum_{L_z S_z s_3 s_4} \sum_{il} \int \frac{d^3 \vec{q}_3}{(2\pi)^3 2q_3^0} \\
&\times \delta(q_3^0 - \frac{\vec{q}_3^2}{2m_c}) Y_{L_\psi L_{\psi z}}^*(\hat{q}_3) \langle s_1; s_2 | S_\psi S_{\psi z} \rangle \langle L_\psi L_{\psi z}; S_\psi S_{\psi z} | J_\psi J_{\psi z} \rangle \langle 3j; \bar{3}k | 1 \rangle \\
&\times \int \frac{d^3 \vec{q}_4}{(2\pi)^3 2q_4^0} \delta(q_4^0 - \frac{\vec{q}_4^2}{2m_c}) Y_{LL_z}^*(\hat{q}_4) \langle s_3; s_4 | S S_z \rangle \langle LL_z; S S_z | J J_z \rangle \langle 3l; \bar{3}i | 1 \rangle \\
&\times \mathcal{A}(a + b \rightarrow Q_j(\frac{P_3}{2} + q_3) + \bar{Q}_k(\frac{P_3}{2} - q_3) + Q_l(\frac{P_4}{2} + q_4) + \bar{Q}_i(\frac{P_4}{2} - q_4)),
\end{aligned} \tag{1}$$

where $\langle 3j; \bar{3}k | 1 \rangle = \delta_{jk}/\sqrt{N_c}$ and $\langle 3l; \bar{3}i | 1 \rangle = \delta_{li}/\sqrt{N_c}$, $\langle s_1; s_2 | S_\psi S_{\psi z} \rangle$ and $\langle s_3; s_4 | SS_z \rangle$, $\langle L_\psi L_{\psi z}; S_\psi S_{\psi z} | J_\psi J_{\psi z} \rangle$ and $\langle LL_z; SS_z | JJ_z \rangle$ are respectively the color-SU(3), spin-SU(2), and angular momentum Clebsch-Gordan coefficients for $Q\bar{Q}$ pairs projecting out appropriate bound states.

After integrating over the relative momenta q_3 and q_4 , we get

$$\begin{aligned} \mathcal{A}(a + b \rightarrow Q\bar{Q}(^{2S_\psi+1}L_{J_\psi})(P_3) + Q\bar{Q}(^{2S+1}L_J)(P_4)) &= \sqrt{C_{L_\psi}}\sqrt{C_L} \sum_{L_\psi S_\psi} \sum_{s_1 s_2} \sum_{jk} \sum_{L_z S_z} \sum_{s_3 s_4} \sum_{il} \\ &\times \langle s_1; s_2 | S_\psi S_{\psi z} \rangle \langle L_\psi L_{\psi z}; S_\psi S_{\psi z} | J_\psi J_{\psi z} \rangle \langle 3j; \bar{3}k | 1 \rangle \\ &\times \langle s_3; s_4 | SS_z \rangle \langle LL_z; SS_z | JJ_z \rangle \langle 3l; \bar{3}i | 1 \rangle \\ &\times \begin{cases} \mathcal{A}(a + b \rightarrow Q_j(\frac{P_3}{2}) + \bar{Q}_k(\frac{P_3}{2}) + Q_l(\frac{P_4}{2}) + \bar{Q}_i(\frac{P_4}{2})) & (L = S), \\ \epsilon_\alpha^*(L_Z) \mathcal{A}^\alpha(a + b \rightarrow Q_j(\frac{P_3}{2}) + \bar{Q}_k(\frac{P_3}{2}) + Q_l(\frac{P_4}{2}) + \bar{Q}_i(\frac{P_4}{2})) & (L = P), \end{cases} \end{aligned} \quad (2)$$

where the coefficients C_{L_ψ} and C_L can be related to the radial wave function of the bound states $R_{nl}^{(l)}(0)$ as

$$C_S = \frac{1}{4\pi} |R_S(0)|^2, \quad C_P = \frac{3}{4\pi} |R'_P(0)|^2. \quad (3)$$

We introduce the spin projection operators $P_{SS_z}(P, q)$ as

$$P_{SS_z}(P, q) \equiv \sum_{s_1 s_2} \langle s_1; s_2 | SS_z \rangle v(\frac{P}{2} + q; s_1) \bar{u}(\frac{P}{2} - q; s_2). \quad (4)$$

Expanding $P_{SS_z}(P, q)$ in terms of the relative momentum q , we get the projection operators and their derivatives, which will be used in our calculation, as follows

$$P_{1S_z}(P, 0) = \frac{1}{2\sqrt{2}} \not{\epsilon}^*(S_z)(\not{P} + 2m_c). \quad (5)$$

$$P_{00}(P, 0) = \frac{1}{2\sqrt{2}} \gamma_5(\not{P} + 2m_c). \quad (6)$$

$$P_{1S_z}^\alpha(P, 0) = \frac{1}{2\sqrt{2}m_c} [\gamma^\alpha \not{\epsilon}^*(S_z)(\not{P} + 2m_c) - (\not{P} - 2m_c) \not{\epsilon} \gamma^\alpha]. \quad (7)$$

Then one can calculate the cross sections for the on-shell quarks in the factorized form of NRQCD[1]. The cross section for $e^+ + e^- \rightarrow J/\psi + \eta_c$ process in Fig. 1 is given by

$$\sigma(a(p_1) + b(p_2) \rightarrow J/\psi(P_3) + \eta_c(P_4)) = \frac{2\pi\alpha^2\alpha_s^2 |R_s(0)|^4 \sqrt{s - 16m_c^2}}{81m_c^2 s^{3/2}} \int_{-1}^1 |\bar{M}|^2 d\cos\theta, \quad (8)$$

where

$$|\bar{M}|^2 = \frac{-16384m_c^2(32m_c^4 - t^2 - u^2)}{s^5}. \quad (9)$$

The Mandelstam variables are defined as

$$s = (p_1 + p_2)^2, \quad (10)$$

$$t = (p_3 - p_1)^2, \quad (11)$$

$$u = (p_3 - p_2)^2. \quad (12)$$

The cross section for $e^+ + e^- \rightarrow J/\psi + \chi_{cJ}$ process is

$$\sigma(a(p_1) + b(p_2) \rightarrow J/\psi(P_3) + \chi_{cJ}(P_4)) = \frac{2\pi\alpha^2\alpha_s^2|R_s(0)|^2|R'_p(0)|^2\sqrt{s-16m_c^2}}{27m_c^2s^{3/2}} \int_{-1}^1 |\bar{M}_J|^2 d\cos\theta, \quad (13)$$

where $|\bar{M}_J|^2$ for χ_{c0} , χ_{c1} and χ_{c2} are given by

$$\begin{aligned} |\bar{M}_0|^2 = & 2048(90112m_c^{10} - 74752m_c^8t - 74752m_c^8u + 23360m_c^6t^2 + 43136m_c^6tu + 23360m_c^6u^2 \\ & - 3152m_c^4t^3 - 7600m_c^4t^2u - 7600m_c^4tu^2 - 3152m_c^4u^3 + 162m_c^2t^4 + 444m_c^2t^3u \\ & + 564m_c^2t^2u^2 + 444m_c^2tu^3 + 162m_c^2u^4 - t^4u - 3t^3u^2 - 3t^2u^3 - tu^4)/(3s^7m_c^2), \end{aligned} \quad (14)$$

$$\begin{aligned} |\bar{M}_1|^2 = & 32768(1792m_c^8 + 256m_c^6t + 256m_c^6u - 56m_c^4t^2 - 64m_c^4tu - 56m_c^4u^2 - 4m_c^2t^3 \\ & - 20m_c^2t^2u - 20m_c^2tu^2 - 4m_c^2u^3 + t^4 + 2t^3u + 2t^2u^2 + 2tu^3 + u^4)/s^7, \end{aligned} \quad (15)$$

$$\begin{aligned} |\bar{M}_2|^2 = & 4096(145408m_c^{10} - 1024m_c^8t - 1024m_c^8u - 2368m_c^6t^2 - 6400m_c^6tu - 2368m_c^6u^2 \\ & + 16m_c^4t^3 - 208m_c^4t^2u - 208m_c^4tu^2 + 16m_c^4u^3 + 24m_c^2t^4 + 72m_c^2t^3u + 96m_c^2t^2u^2 \\ & + 72m_c^2tu^3 + 24m_c^2u^4 - t^4u - 3t^3u^2 - 3t^2u^3 - tu^4)/(3s^7m_c^2). \end{aligned} \quad (16)$$

In the numerical calculations, we chose $\sqrt{s} = 10.6\text{GeV}$, $m_c = 1.5\text{GeV}$, $\alpha_s = 0.26$, $|R_s(0)|^2 = 0.810\text{GeV}^3$ and $|R'_p(0)|^2 = 0.075\text{GeV}^5$ [9], and assume that in the non-relativistic approximation $m_{J/\psi} = m_{\eta_c} = m_{\chi_c} = 2m_c$. The numerical result for $e^+e^- \rightarrow J/\psi\eta_c$ is

$$\sigma(e^+e^- \rightarrow J/\psi\eta_c) = 5.5fb. \quad (17)$$

While the numerical result for the cross section of $e^+e^- \rightarrow J/\psi\eta_c$ is more than a factor of six smaller than the experimental data[2] (with uncertainties due to the unknown decay branching fractions into 4-charged particles for the η_c), the calculated ratio of $\sigma(e^+e^- \rightarrow J/\psi\eta_c)/\sigma(e^+e^- \rightarrow J/\psi c\bar{c}) \approx 0.079$ might be consistent with the experimental result with the choice of $\sigma(e^+e^- \rightarrow J/\psi c\bar{c}) = 70\text{fb}$ [6, 7, 8].

The cross sections for $J/\psi\chi_{cJ}$ production are given as

$$\sigma(e^+e^- \rightarrow J/\psi\chi_{c0}) = 6.7fb, \quad (18)$$

$$\sigma(e^+e^- \rightarrow J/\psi\chi_{c1}) = 1.1fb, \quad (19)$$

$$\sigma(e^+e^- \rightarrow J/\psi\chi_{c2}) = 1.6fb. \quad (20)$$

In Fig. 2, we see that the cross sections for $e^+e^- \rightarrow J/\psi\eta_c$, $e^+e^- \rightarrow J/\psi\chi_{c1}$ and $e^+e^- \rightarrow J/\psi\chi_{c2}$ decrease rapidly as the e^+e^- center-of-mass energy \sqrt{s} increases, but the one for χ_{c2} is slower than η_c and χ_{c1} .

If we choose $\sigma(e^+e^- \rightarrow \chi_{c1}c\bar{c}) = 18.1fb$ and $\sigma(e^+e^- \rightarrow \chi_{c2}c\bar{c}) = 8.4fb$ which were obtained in the fragmentation approximation [11], then we have the ratio

$$\sigma(e^+e^- \rightarrow J/\psi\chi_{c1})/\sigma(e^+e^- \rightarrow \chi_{c1}c\bar{c}) = 0.061, \quad (21)$$

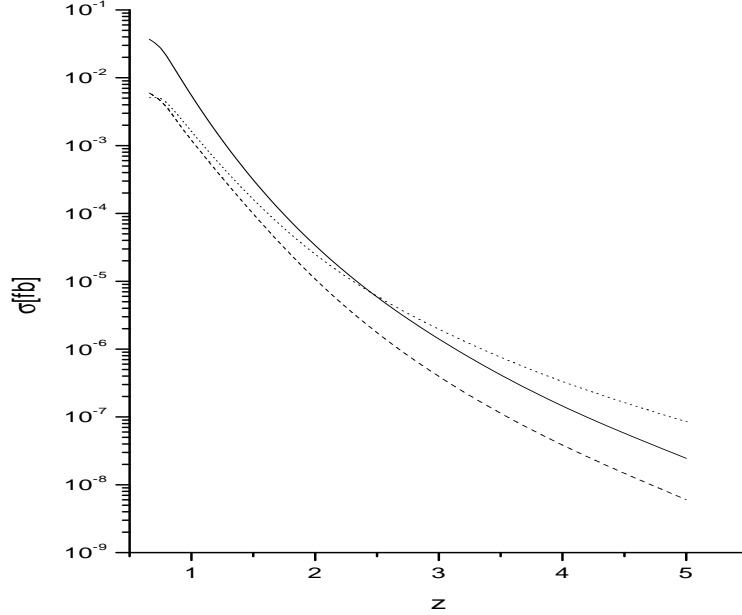


Figure 2: Cross sections for $\sigma(e^+e^- \rightarrow J/\psi\eta_c)$ (solid line) and $\sigma(e^+e^- \rightarrow J/\psi\chi_{cJ})$ (dashed line for $J = 1$, dotted line for $J = 2$) plotted against the e^+e^- center-of -mass energy \sqrt{s} with $z=\sqrt{s/s_0}$ and $\sqrt{s_0} = 10.6\text{GeV}$.

$$\sigma(e^+e^- \rightarrow J/\psi\chi_{c2})/\sigma(e^+e^- \rightarrow \chi_{c2}c\bar{c}) = 0.19. \quad (22)$$

As for the χ_{c0} , in Ref. [3] $\sigma(e^+e^- \rightarrow \chi_{c0}c\bar{c})=5.0$ fb was obtained in the fragmentation approximation. It is puzzling that this inclusive production cross section is even smaller than the exclusive cross section given in Eq. (18). In order to clarify this problem here we recalculate $\sigma(e^+e^- \rightarrow \chi_{c0}c\bar{c})$ in a complete form to the $\mathcal{O}(\alpha_s^2)$ order in perturbative QCD.

We give the amplitude of the first diagram in Fig. 3 for $e^+e^- \rightarrow \chi_{c0}c\bar{c}$ as

$$M = \sum_{L_z S_z} \sigma_\alpha^*(L_z) \langle 1L_z; 1S_z | J = 0, J_z = 0 \rangle = \frac{ie_c e g_s^2 [T^a T^a]_{li}}{\sqrt{3}} \bar{v}(p_1) \gamma^\mu u(p_2) \frac{1}{s} \bar{u}_l(p_c) \\ \times [\gamma^\alpha P_{1S_z} \gamma_\alpha(p, 0) \mathcal{O}_\mu^\sigma + \gamma^\alpha P_{1S_z}^\sigma \gamma_\alpha \mathcal{O}_\mu] v_i(p_{\bar{c}}), \quad (23)$$

where $e_c = \frac{2}{3}e$, T^a is the $SU(3)$ color matrix, the matrix \mathcal{O}_μ is relevant to the on shell amplitude and \mathcal{O}_μ^σ is its derivative of the relative momentum between the quarks that form the bound state. The contributions of other three diagrams are similar. Some useful information of the calculation is given in the Appendix.

We finally get the cross section for this process

$$\sigma(e^+e^- \rightarrow \chi_{c0}c\bar{c}) = 9.2fb, \quad (24)$$

which is larger than that given in Ref. [3] under the fragmentation approximation.

Using $\sigma(e^+e^- \rightarrow \chi_{c0}c\bar{c}) = 9.2fb$ and Eq. (18) we get

$$\sigma(e^+e^- \rightarrow \chi_{c0}J/\psi)/\sigma(e^+e^- \rightarrow \chi_{c0}c\bar{c}) = 0.73. \quad (25)$$

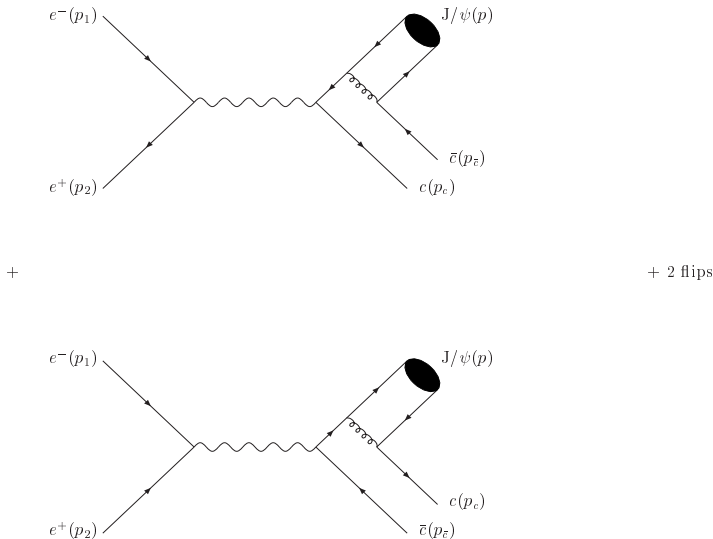


Figure 3: Feynman diagrams for $e^+ + e^- \rightarrow \chi_{c0} + c\bar{c}$ process.

The ratio in Eq. (25) would mean that $\sigma(e^+e^- \rightarrow \chi_{c0}J/\psi)$ plus $\sigma(e^+e^- \rightarrow \chi_{c0}\psi(2S))$ will saturate the χ_{c0} inclusive production cross section. This is not reasonable because the $D\bar{D}$ meson pair associated with χ_{c0} should have a high production rate [2]. This indicates that the perturbative QCD calculation for inclusive double charm production seriously underestimates the rate at low energies such as $\sqrt{s} = 10.6\text{GeV}$. In Fig. 4, we show cross sections for $\sigma(e^+e^- \rightarrow \chi_{c0}c\bar{c})$ (solid line) and $\sigma(e^+e^- \rightarrow J/\psi\chi_{c0})$ (dotted line) plotted against the e^+e^- center-of-mass energy \sqrt{s} with $z = \sqrt{s/s_0}$ and $\sqrt{s_0} = 10.6\text{GeV}$. One can see the ratio Eq. (25) decreases drastically as the center-of-mass energy increases. The ratio is 2.4×10^{-3} at $\sqrt{s} = 32\text{GeV}$ and 1.5×10^{-4} at $\sqrt{s} = 53\text{GeV}$, where the associated $D\bar{D}$ meson pair production is expected to dominate. This may imply that the perturbative QCD calculation for double charm production might become reliable only when the e^+e^- center-of-mass energy is much larger than the static energies of the four charm quarks created in this process. The χ_{c0} double charm inclusive production may serve as a good example to show the limited applicability of perturbative QCD at lower energies such as $\sqrt{s} = 10.6\text{GeV}$.

In summary, despite of many uncertainties due to the relativistic corrections, the QCD radiative corrections, the possible color-octet channel contributions, and the physical parameters (e.g. the charm quark mass and the strong coupling constant), both the inclusive and exclusive double charm production cross sections calculated in perturbative QCD turned out to be seriously underestimated. Therefore we intend to conclude, as in [3], that it is hard to explain the double charm production data observed by Belle based on perturbative QCD (including both color-singlet and color-octet channels), and possible nonperturbative QCD effects have to be considered at $\sqrt{s} = 10.6\text{GeV}$.

While we were about to submit our result, there appeared one paper which also con-

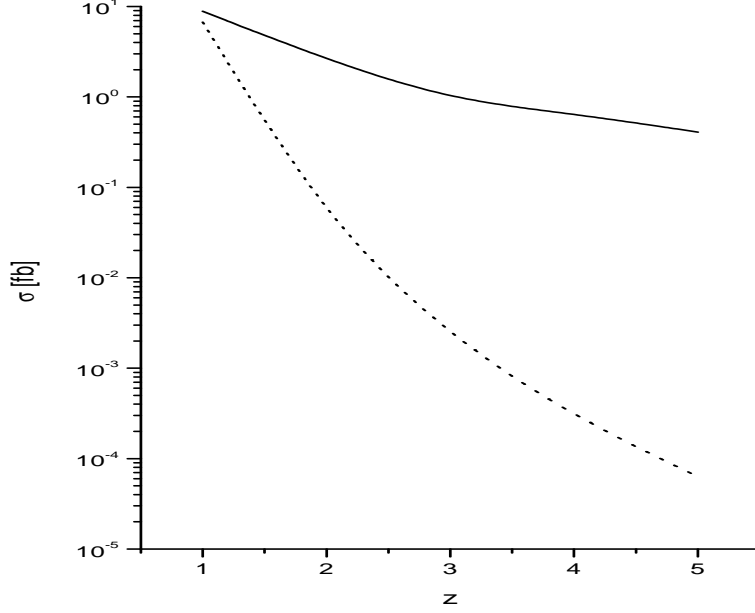


Figure 4: cross sections for $\sigma(e^+e^- \rightarrow \chi_{c0}c\bar{c})$ (solid line) and $\sigma(e^+e^- \rightarrow J/\psi\chi_{c0})$ (dotted line) plotted against the e^+e^- center-of -mass energy \sqrt{s} with $z=\sqrt{s/s_0}$ and $\sqrt{s_0} = 10.6\text{GeV}$.

sidered exclusive double-charmonium production[12]. Those authors took the QED effects into account in addition to the QCD effects that we considered. We find our result for the exclusive double-charmonium production is consistent with theirs but we also analyzed the inclusive processes which were not discussed in Ref. [12].

Acknowledgments

The authors thank L.K. Hao and Z.Z. Song for useful discussions. We also thank C.F. Qiao for useful comments. This work was supported in part by the National Natural Science Foundation of China, and the Education Ministry of China.

Appendix

In this appendix we give the cross section for the $e^+e^- \rightarrow \chi_{c0}c\bar{c}$ process in Fig. 3.

$$d\sigma = \frac{|\bar{M}|^2}{2s(2\pi)^5} \delta^4(p_1 + p_2 - p_c - p_{\bar{c}} - p) \frac{d^3p_c}{2E_c} \frac{d^3p_{\bar{c}}}{2E_{\bar{c}}} \frac{d^3p}{2E}. \quad (26)$$

It is convenient to rewrite the cross section as

$$\begin{aligned} d\sigma &= \frac{|\bar{M}|^2}{2s(2\pi)^5} \delta^4(p_1 + p_2 - \eta - p) \delta^4(\eta - p_c - p_{\bar{c}}) \frac{d^3p_c}{2E_c} \frac{d^3p_{\bar{c}}}{2E_{\bar{c}}} \frac{d^3p}{2E} d^4\eta \\ &= \frac{|\bar{M}|^2}{2s(2\pi)^5} \delta^4(p_1 + p_2 - \eta - p) \delta^4(\eta - p_c - p_{\bar{c}}) \frac{d^3p_c}{2E_c} \frac{d^3p_{\bar{c}}}{2E_{\bar{c}}} \frac{d^3p}{2E} \frac{d^3\eta}{2E_\eta} dm_\eta^2, \end{aligned}$$

(27)

where $m_\eta^2 = \eta^2$.

The integral over the phase-space of $c\bar{c}$ is evaluated in the corresponding center of mass frame

$$\frac{d^3 p'_c}{2E'_c} \frac{d^3 p'_{\bar{c}}}{2E'_{\bar{c}}} \delta^4(\eta' - p'_c - p'_{\bar{c}}) = \frac{1}{8m_\eta^2} \lambda^{1/2}(m_\eta^2, m_c^2, m_{\bar{c}}^2) d\Omega', \quad (28)$$

where $\lambda^{1/2}(m_\eta^2, m_c^2, m_{\bar{c}}^2) = \eta^4 + m_c^4 + m_{\bar{c}}^4 - 2m_\eta^2 m_c^2 - 2m_\eta^2 m_{\bar{c}}^2 - 2m_c^2 m_{\bar{c}}^2$.

The remaining integration are performed in the center of mass frame of the e^+e^-

$$\frac{d^3 p}{2E} \frac{d^3 \eta}{2E_\eta} \delta^4(p_1 + p_2 - \eta - p) = \frac{1}{8s} \lambda^{1/2}(s, m_\eta^2, m_p^2) d\Omega. \quad (29)$$

Finally we have

$$d\sigma = \frac{|\bar{M}|^2 C_P}{64s^2 (2\pi)^5 m_\eta m_c} \lambda^{1/2}(m_\eta^2, m_c^2, m_{\bar{c}}^2) \lambda^{1/2}(m_\eta^2, m_c^2, m_{\bar{c}}^2) d\Omega' d\Omega dm_\eta. \quad (30)$$

The limit of m_η is

$$m_c + m_{\bar{c}} \leq m_\eta \leq \sqrt{s} - m_p. \quad (31)$$

To accomplish the integration we use the Lorentz transformation between the two frames as $L = R_2 R_1$, where

$$R_1 = \begin{pmatrix} \sqrt{1 + \frac{\vec{p}^2}{m_\eta^2}} & 0 & 0 & -\frac{|\vec{p}|}{m_\eta} \\ 0 & 1 & 0 & 0 \\ 0 & 0 & 1 & 0 \\ -\frac{|\vec{p}|}{m_\eta} & 0 & 0 & \sqrt{1 + \frac{\vec{p}^2}{m_\eta^2}} \end{pmatrix}. \quad (32)$$

$$R_2 = \begin{pmatrix} 1 & 0 & 0 & 0 \\ 0 & \cos(\theta) & 0 & \sin(\theta) \\ 0 & 0 & 1 & 0 \\ 0 & -\sin(\theta) & 0 & \cos(\theta) \end{pmatrix}. \quad (33)$$

The momenta in the center mass frame of e^+e^- are

$$p_1 = (\sqrt{s}/2, 0, 0, \sqrt{s}/2), \quad (34)$$

$$p_2 = (\sqrt{s}/2, 0, 0, -\sqrt{s}/2), \quad (35)$$

$$p_c = R_2 R_1 p'_c, \quad (36)$$

$$p_{\bar{c}} = R_2 R_1 p'_{\bar{c}}, \quad (37)$$

$$p = (\sqrt{\bar{p}^2 + m_p^2}, |\bar{p}| \sin(\theta), 0, |\bar{p}| \cos(\theta)), \quad (38)$$

where p'_c and $p'_{\bar{c}}$ are the momenta of c and \bar{c} in the Ω' frame, and they are

$$p'_c = (E'_c, |\vec{p}'_c| \sin(\theta') \cos(\theta'), |\vec{p}'_c| \sin(\theta') \cos(\theta'), |\vec{p}'_c| \cos(\theta')), \quad (39)$$

$$p'_{\bar{c}} = (E'_{\bar{c}}, -|\vec{p}'_{\bar{c}}| \sin(\theta') \cos(\theta'), -|\vec{p}'_{\bar{c}}| \sin(\theta') \cos(\theta'), -|\vec{p}'_{\bar{c}}| \cos(\theta')). \quad (40)$$

In Fig. 3 the lower diagrams give very small contributions, so we only keep the upper diagrams and give

$$|\bar{M}|^2 = \frac{2(4\pi)^4 \alpha^2 \alpha_s^2}{27} (aa + 2ab + bb). \quad (41)$$

We define $pp_1 = p \cdot p_1$, $pp_2 = p \cdot p_2$, $pp_3 = p \cdot p_c$, $pp_4 = p \cdot p_{\bar{c}}$, $p_{13} = p_1 \cdot p_c$, $p_{14} = p_1 \cdot p_{\bar{c}}$, $p_{23} = p_2 \cdot p_c$, $p_{24} = p_2 \cdot p_{\bar{c}}$. We also notify $aa=bb$ with

$$\begin{aligned} aa = & (4(800m^{10}s + 800m^8 p_{14}pp_2 + 800m^8 p_{24}pp_1 + 1440m^8 pp_3s + 160m^6 p_{13}p_{24}pp_3 \\ & + 160m^6 p_{14}p_{23}pp_3 + 1440m^6 p_{14}pp_2pp_3 + 1440m^6 p_{24}pp_1pp_3 + 900m^6 pp_3^2s \\ & + 184m^4 p_{13}p_{24}pp_3^2 + 184m^4 p_{14}p_{23}pp_3^2 + 856m^4 p_{14}pp_2pp_3^2 + 856m^4 p_{24}pp_1pp_3^2 \\ & + 216m^4 pp_3^3s + 56m^2 p_{13}p_{24}pp_3^3 + 56m^2 p_{14}p_{23}pp_3^3 + 168m^2 p_{14}pp_2pp_3^3 \\ & + 168m^2 p_{24}pp_1pp_3^3 + 13m^2 pp_3^4s + 2p_{13}p_{24}pp_3^4 + 2p_{14}p_{23}pp_3^4) / (3m^2 s^2 (64m^{12} \\ & + 192m^{10}pp_3 + 240m^8 pp_3^2 + 160m^6 pp_3^3 + 60m^4 pp_3^4 + 12m^2 pp_3^5 + pp_3^6)). \end{aligned} \quad (42)$$

$$\begin{aligned} ab = & (4(400m^{10}s + 400m^8 p_{13}pp_2 + 400m^8 p_{14}pp_2 + 400m^8 p_{23}pp_1 + 400m^8 p_{24}pp_1 \\ & + 400m^8 pp_1pp_2 + 480m^8 pp_3s + 400m^8 pp_{34}s + 480m^8 pp_4s + 80m^6 p_{13}p_{24}pp_3 \\ & + 80m^6 p_{13}p_{24}pp_4 + 280m^6 p_{13}pp_2pp_3 + 440m^6 p_{13}pp_2pp_4 + 80m^6 p_{14}p_{23}pp_3 \\ & + 80m^6 p_{14}p_{23}pp_4 + 440m^6 p_{14}pp_2pp_3 + 280m^6 p_{14}pp_2pp_4 + 280m^6 p_{23}pp_1pp_3 \\ & + 440m^6 p_{23}pp_1pp_4 + 440m^6 p_{24}pp_1pp_3 + 280m^6 p_{24}pp_1pp_4 + 240m^6 pp_1pp_2pp_3 \\ & - 400m^6 pp_1pp_2pp_{34} + 240m^6 pp_1pp_2pp_4 + 140m^6 pp_3^2s + 240m^6 pp_3pp_{34}s \\ & + 476m^6 pp_3pp_4s + 240m^6 pp_{34}pp_4s + 140m^6 pp_4^2s + 40m^4 p_{13}p_{24}pp_3^2 + 104m^4 p_{13}p_{24}pp_3pp_4 \\ & + 40m^4 p_{13}p_{24}pp_4^2 + 20m^4 p_{13}pp_2pp_3^2 + 288m^4 p_{13}pp_2pp_3pp_4 + 120m^4 p_{13}pp_2pp_4^2 \\ & + 40m^4 p_{14}p_{23}pp_3^2 + 104m^4 p_{14}p_{23}pp_3pp_4 + 40m^4 p_{14}p_{23}pp_4^2 + 120m^4 p_{14}pp_2pp_3^2 \\ & + 288m^4 p_{14}pp_2pp_3pp_4 + 20m^4 p_{14}pp_2pp_4^2 + 20m^4 p_{23}pp_1pp_3^2 + 288m^4 p_{23}pp_1pp_3pp_4 \\ & + 120m^4 p_{23}pp_1pp_4^2 + 120m^4 p_{24}pp_1pp_3^2 + 288m^4 p_{24}pp_1pp_3pp_4 + 20m^4 p_{24}pp_1pp_4^2 \\ & - 240m^4 pp_1pp_2pp_3pp_{34} + 144m^4 pp_1pp_2pp_3pp_4 - 240m^4 pp_1pp_2pp_{34}pp_4 + 108m^4 pp_3^2pp_4s \\ & + 144m^4 pp_3pp_{34}pp_4s + 108m^4 pp_3pp_4^2s + 28m^2 p_{13}p_{24}pp_3^2pp_4 + 28m^2 p_{13}p_{24}pp_3pp_4^2 \\ & + 12m^2 p_{13}pp_2pp_3^2pp_4 + 72m^2 p_{13}pp_2pp_3pp_4^2 + 28m^2 p_{14}p_{23}pp_3^2pp_4 + 28m^2 p_{14}p_{23}pp_3pp_4^2 \end{aligned}$$

$$\begin{aligned}
& +72m^2 p_{14} p p_2 p p_3^2 p p_4 + 12m^2 p_{14} p p_2 p p_3 p p_4^2 + 12m^2 p_{23} p p_1 p p_3^2 p p_4 + 72m^2 p_{23} p p_1 p p_3 p p_4^2 \\
& +72m^2 p_{24} p p_1 p p_3^2 p p_4 + 12m^2 p_{24} p p_1 p p_3 p p_4^2 - 144m^2 p p_1 p p_2 p p_3 p p_3 p p_4 + 13m^2 p p_3^2 p p_4^2 s \\
& +2p_{13} p_{24} p p_3^2 p p_4^2 + 2p_{14} p_{23} p p_3^2 p p_4^2) / (3m^2 s^2 (64m^{12} + 96m^{10} p p_3 + 96m^{10} p p_4 + 48m^8 p p_3^2 \\
& +144m^8 p p_3 p p_4 + 48m^8 p p_4^2 + 8m^6 p p_3^3 + 72m^6 p p_3^2 p p_4 + 72m^6 p p_3 p p_4^2 + 8m^6 p p_4^3 \\
& +12m^4 p p_3^3 p p_4 + 36m^4 p p_3^2 p p_4^2 + 12m^4 p p_3 p p_4^3 + 6m^2 p p_3^3 p p_4^2 + 6m^2 p p_3^2 p p_4^3 + p p_3^3 p p_4^3)). \quad (43)
\end{aligned}$$

References

- [1] G.T. Bodwin, L. Braaten, and G.P. Lepage, Phys. Rev. **D51**, 1125 (1995).
- [2] Belle Collaboration, K. Abe *et al.*, hep-ex/0205104.
- [3] K.T. Chao and L.K. Hao, hep-ph/0209189.
- [4] G.L. Kane, J.P. Leveille and D.M. Scott, Phys. Lett. **B85**, 115 (1979).
- [5] S.J. Brodsky, C.R. Ji, Phys. Rev. Lett. **55**, 2257 (1985).
- [6] P. Cho and A.K. Leibovich, Phys. Rev. **D53**, 150 (1996); 53, 6203 (1996). S. Baek, P. Ko, J. Lee and H.S. Song, J. Kor. Phys. Soc. **33**, 97 (1998); hep-hp/9804455.
- [7] F. Yuan, C.F. Qiao and K.T. Chao, Phys. Rev. **D56**, 321 (1997).
- [8] V.V. Kiselev, A.K. Likhoded and M.V. Shevlyagin, Phys. Lett. **B332**, 411 (1994).
- [9] E.J. Eichten and C. Quigg, Phys. Rev. **D52**, 1726 (1995).
- [10] Belle Collaboration, K. Abe *et al.*, Phys. Rev. Lett. **88** 052001 (2002)
- [11] G.A. Schuler and M. Vanttinen, Phys. Rev. **D58**, 017502 (1998).
- [12] E. Braaten and J. Lee, hep-ph/0211085.